 doi:10.20944/preprints202009.0023.v1

Article

Application of the incremental modal analysis for bridges (IMPAb) subjected to near-fault ground motions

Alessandro Vittorio Bergami[1,*], Gabriele Fiorentino[1], Davide Lavorato[1], Bruno Briseghella[2] and Camillo Nuti [1,2]

[1] Department of Architecture, Roma Tre University, 00152 Rome, Italy; alessandro.bergami@uniroma3.it (A.V.B.); gabriele.fiorentino@uniroma3.it (G.F.); camillo.nuti@uniroma3.it (C.N.); davide.lavorato@uniroma3.it (D.L.);
[2] College of Civil Engineering, Fuzhou University; bruno@fzu.edu.cn
* Correspondence: alessandro.bergami@uniroma3.it; Tel.: +39-(06)-57332907

Abstract: Near-fault ground motions can cause severe damage to civil structures, including bridges. Safety assessment of these structures for near fault ground motion is usually performed through Non-Linear Dynamic Analyses, while faster methods are often used. IMPAb (Incremental Modal Pushover Analysis for Bridges) permits to investigate the seismic response of a bridge by considering the effects of higher modes, which are often relevant for bridges. In this work, IMPAb is applied to a bridge case study considering near-fault pulse-like ground motion records. The records were analyzed and selected from the European Strong Motion Database and the pulse parameters were evaluated. In the paper results from standard pushover procedures and IMPAb are compared with nonlinear Response-History Analysis (NRHA), considering also the vertical component of the motion, as benchmark solutions and incremental dynamic analysis (IDA). Results from the case study demonstrate that the vertical seismic action has a minor influence on the structural response of the bridge. Therefore IMPAbremains very effective conserving the original formulation of the procedure, and can be considered a well performing procedure also for near-fault events.

Keywords: near field, pulse like ground motions, bridge, non-linear static analysis, non-linear dynamic analysis

1. Introduction

Near-field ground motions (NF) are different from ordinary (far field) ground motions as the proximity to the fault renders the effect of the global displacements and the mutual displacements of the opposite sides of the fault very evident in the records: i) the vertical motion component maximum values often exceeds the horizontal component [1]; ii) long period velocity pulses can be generated by earthquake directivity and iii) long period velocity pulsescan be generated by earthquake fling-step [2], iv) differential input displacements at the base of the piers [3].

For i), in structures sensible to axial force variation, the combined effect of horizontal and vertical motions can bring to severe structural demand [4].

Case ii) happens due to the focusing of wave energy along the fault in the direction of rupture, when the fault rupture propagates towards the site (forward directivity) and when the velocity of propagation is slightly slower than the shear wave velocity, causing the seismic energy to arrive in a large pulse of motion [5]. In this case the pulses in the velocity time series are generally double-sided, and they are stronger on the component of motion normal to the fault strike.

Case iii) (Fling-step) occurs when the earthquake causes major surface rupture. In this case, there is a slow build-up of stresses in the earth's crust over long periods of time, that then are quickly

 doi:10.20944/preprints202009.0023.v1

released causing a permanent offset in the displacement time series [6]. Fling-step effects produce single-sided pulses. For dip-slip faults, also these effects are observed in the component of motion normal to the fault strike.

Case iv), differential displacements, will not be treated here even though the authors discussed possible input generations and relative effects in various publications [7, 30].

Near Fault effect on Bridges are usually investigated by means of Non-Linear Response History Analyses (NRHA) [8-11]. Consequently, a method frequently used to assess the response of structures to NF is the Incremental Dynamic Analysis (IDA) [12], which uses a set of ground motion records and requires to execute several NRHA. NRHA allows to properly estimate the seismic demand and capacity of structures considering each component of the seismic action: horizontal and vertical (the vertical component is relevant for NF events).

Due to the long analysis time and complexity required to perform several NRHA and to the specific complexity of the dynamic method, it is useful to investigate alternative static methods which can provide results with lower computational effort. For the previous reasons, some authors proposed the use of pushover analyses to investigate the response of bridge structures under near fault seismic input [13,14].

In [15-17], the authors of this paper proposed an incremental (in terms of seismic intensity) pushover-based procedure (specifically developed for bridges) named IMPAb, and discussed the validity in case of far field accelerograms (FF). The procedure employs the envelope of a single-run conventional uniform pushover analysis (UPA) and modal pushover analyses (MPA), to determine the seismic demands for each intensity level considered,.

In case of NF ground motions the vertical action becomes relevant, therefore its consideration or neglection should be discussed. In this work this issue has been considered and the necessity of performing vertical and horizontal pushover has been evaluated testing the IMPAb procedure substituting MPA with the Extended Modal Pushover Analysis (EMPA) [19], which considers the 3D components of the accelerograms. Nonetheless, the prediction of the structural response of the bridge with EMPA, also for NF events, is close to MPA (the same conclusion is discussed in [19] for the case study performed) and therefore the original version of IMPAb, developed and tested considering far-field ground motions (FF), was tested and discussed herein and validated in case of NF.

The main task of this work is to apply IMPAb procedure using a set of near-fault ground motion records as input. In the present paper the same case study of irregular bridge selected in [17] was analyzed.

In the paper the seismic demands resulting from IMPAb are compared to those predicted from incremental dynamic analysis (IDA) as a benchmark solution. Therefore, according to IDA, several nonlinear time-history analysis have been performed considering a set of near-fault ground motions (both horizonal and vertical components have been considered) whereas, performing IMPAb, the response spectra of those ground motions have been used for the seismic demand. Several pushover analyses were performed for the bridge and then, a comparison was made between the results obtained according to the single pushover procedure and to the IMPAb with reference to NRHA and IDA. It is worth noting that the spatial variation of motion on the different bridge piers are not taken into account in this work. For this issue, it is possible to make reference to other literature studies [18].

After a short description of IMPAb procedure (**§2**), the case study of the selected bridge will be introduced (**§3.1**), then the selection of the near-fault seismic input will be described (**§3.2**) and the numerical model will be displayed (§3.3). The execution and results of non-linear analyses are given in **§4**, while **§5** and **§6** provide discussion of the results and conclusions.

2. Short description of IMPAb procedure

It is assumed that NRHA represents the "correct" response evaluation, even for NF input. The incremental modal pushover analysis for bridges (IMPAb) [17] is carried out and results compared to IDA's. IMPAb requires the execution of several pushover analyses according to two different load

Preprints (www.preprints.org) | NOT PEER-REVIEWED | Posted: 2 September 2020 doi:10.20944/preprints202009.0023.v1

patterns: a uniform loading profile (UPA) and a modal pushover analysis (MPA) according to the procedure presented in [15,16]. As previously mentioned, the use of EMPA (which includes vertical action) instead of MPA was tested and verified as irrelevant for the scope of the analysis. The irrelevance of the vertical input performing the pushover analysis, according to the scope and the results of this paper, is discussed in section 4.

In addition, in this work a standard pushover (SPA), with a load pattern proportional to the dominant modal shape, has been performed to compare results from different pushover procedures with NRHA. The IMPAb procedure can be summarized in the following main steps:

- Definition of the seismic demand in terms of response spectra (RS) for a defined range of intensity levels;
- Discretization of the intensities range and definition of a set of intensity level I;
- Execution of a traditional pushover analysis adopting a uniform loading profile (UPA);
- Evaluation of the natural frequencies, w_n and modes, n for the linear elastic vibration of the bridge. The modal properties of the bridge model are obtained from the linear dynamic modal analysis in which the relevant modes of the bridge are selected;
- Execution of a modal pushover analysis for each intensity level. For the intensity level i, the performance point (P.P.) for the selected (predominant) modes can be determined and, using a combination rule, the P.P. corresponding to each mode for each intensity i can be combined to derive the "multimodal performance point" (P.P.m,i). The P.P.m,i is expressed in terms of monitoring point displacement u_{rmmi}, and corresponding global base shear $V_{b,i}$, for each intensity level considered: being u_{rmi} the modal displacements of the monitoring point, in this paper the transverse direction has been considered.

Therefore IMPAb requires to perform an incremental modal pushover analysis (IMPA) and an incremental UPA (IUPA). Afterwards to derive an univocal capacity curve from an envelope, in IMPAb the capacity curve is defined connecting, for each intensity step *i*, the performance point $P_{i,IMPAb}$ defined in (1) and described in Figure 1.

$$P_{i,IMPAb} = (\max(u_{r,i,MPA};u_{r,i,UPA});\ \max(V_{b,i,MPA};V_{b,i,UPA})) \quad (1)$$

being $(u_{r,i,MPA};\ V_{b,i,MPA})$ and $(u_{r,i,UPA};\ V_{b,i,UPA})$ the coordinates of the performance point for the intensity "i" obtained performing MPA or UPA. The seismic demand is expressed in terms of Response Spectrum (RS): a RS can be selected and scaled according to different criteria. In the application discussed herein the RS have been derived from the set of near-fault ground motion records selected (§ 3.2). The RS have been linearly scaled to match the desired intensity range.

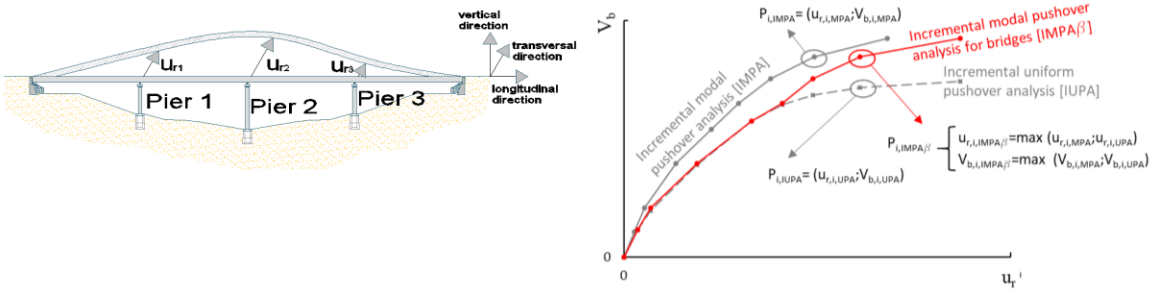

(a) (b)

Figure 1. (a) Degrees of freedom of the bridge: performing a pushover analysis the displacement u_r of the monitoring point is controlled. In this work u_r is the transversal displacement. (b) Evaluation of the IMPAb capacity curve: envelope of IUPA and IMPA.

Preprints (www.preprints.org) | NOT PEER-REVIEWED | Posted: 2 September 2020 doi:10.20944/preprints202009.0023.v1

3. Case study

3.1. The case study

The case study selected is a straight bridge with four equal 50 m spans for a total length of 200m (Figure 2), already used by many authors in previous comparison works since 1990s [21] and also to explain the IMPAb in [17]. The deck of the bridge consists of 14m wide pre-cast concrete box girder supported by piers through bearings locked in the transverse direction and, at the abutments, through elastomeric bearings (movement in the longitudinal direction is allowed at the abutments, but transverse displacements are restrained).

The piers, all consisting of circular cross-section with a 2.5m diameter, have variable heights. The concrete class used was C20/25 (characteristic compressive cylindric strength f_{ck}=20 MPa) while B450C steel (characteristic yield strength f_{yk} = 450MPa) reinforcement was used throughout the structure. The bridge was designed according to Eurocode 8 using a design peak ground acceleration of 0.35g and a behavior factor (coefficient *q)* of 3.0; the design loads are summarized in **Table 1**.

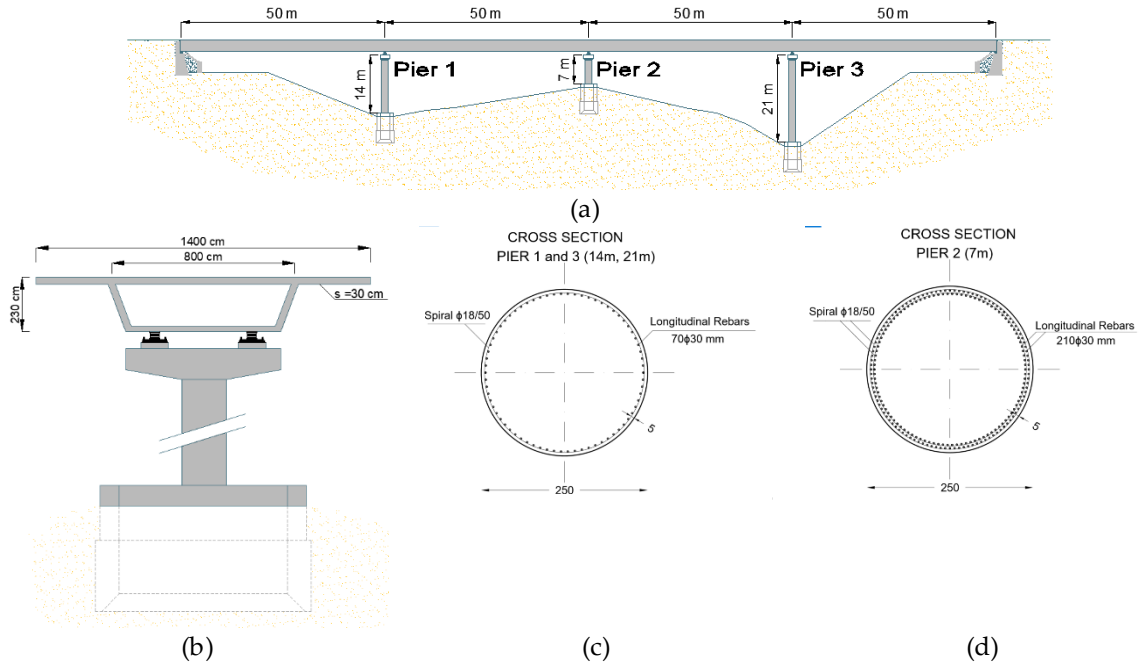

Figure 2. Selected bridge case study: (a) longitudinal view; (b) Bridge Pier elevation view; (c) and (d) Bridge pier sections.

Table 1. Loads and actions.

	Load	kN/m	kN
Dead	Self-weight	200	-
Live	Vehicle loads (Qik)	-	1200
Live	Distributed load (qik)	54.5	-

The response of the bridge model was estimated through the employment of non-linear static and dynamic analyses. The dynamic analyses were performed adopting a set of ground motions (GM) selected according to the criteria described in §3.2; from the set of ground motions a median response spectra (RSm) was defined. The GMs were used to perform the NRHAs as well as their mean spectrum (RSm) was used for the purpose of evaluating the pushover-based procedure (the performance point is evaluated, for each intensity level, adopting RSm for the seismic demand).

Preprints (www.preprints.org) | NOT PEER-REVIEWED | Posted: 2 September 2020 doi:10.20944/preprints202009.0023.v1

In the paper (§4) analysis results are presented in terms of deformed shape of the bridge in transverse direction and plotting the bridge capacity curve (i.e. monitoring point displacement versus seismic intensity).

3.2. Selection of Near Fault Records

The seismic events which hit Italy in 2016 and 2017, known as Central Italy earthquakes, had been a series of four seismic events occurred in Italy between August and October 2016 [22] with minor events in January 2017. The two major earthquakes were those occurred on August 24 and October 30, 2016 with magnitudes Mw = 6 and 6.5, respectively. In both cases, many seismic stations close to the epicenters recorded the strong ground motion. In some cases, the records presented typical near-fault pulse-like behavior, as highlighted both in the joint report written by the ReLUIS-INGV Workgroup [23] and reported in the European Strong Motion Database [24]. **Table 2** reports the ground motion parameters of the selected records for August 24. The Joyner and Boore distance (R_{jb}) is the distance from the fault surface projection, and it is reported together with the epicentral distance (R_{epi}).

Table 2. Ground motion parameters of August 24, 2016 records. Accelerations and velocities are expressed in g and cm/s, respectively. PGA = Peak Ground Acceleration; PGV = Peak Ground Velocity;

Station	R_{epi} (km)	R_{JB} (km)	PGA_EW	PGA_NS	PGA_Z	PGV_EW	PGV_NS	PGV_Z
AMT	8.5	1.4	0.87	0.38	0.40	43.5	41.5	33.7
FEMA	32.9	13.9	0.25	0.19	0.08	14.6	9.2	6.3
MNF	40.3	20.4	0.07	0.04	0.06	4.8	2.9	4.6
NOR	15.6	2.3	0.20	0.18	0.25	27.1	21.1	11.5
NRC	15.3	2.0	0.36	0.37	0.22	29.8	23.7	11.6
RM33	21.1	13.0	0.10	0.10	0.04	9.3	6.2	5.0

The characteristics of the main events were reported by a number of authors. The study by **Luzi et al.** [25] reports, among the other pieces of information, a strike of the causative fault of 156 degrees with respect to the North-South direction for the event of August 24. According to these indications, the horizontal records were rotated in order to obtain the Fault Normal and Fault Parallel components of the ground motion. **Figure 3** reports the Fault Normal components of the acceleration time series of the selected near-fault ground motion records.

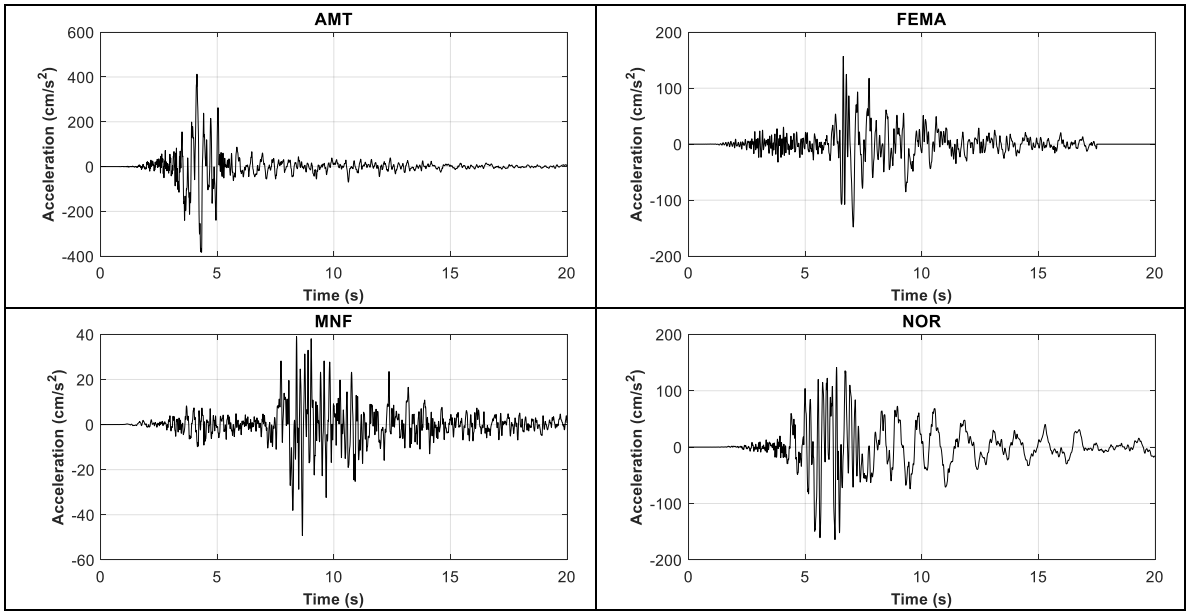

Preprints (www.preprints.org) | NOT PEER-REVIEWED | Posted: 2 September 2020 doi:10.20944/preprints202009.0023.v1

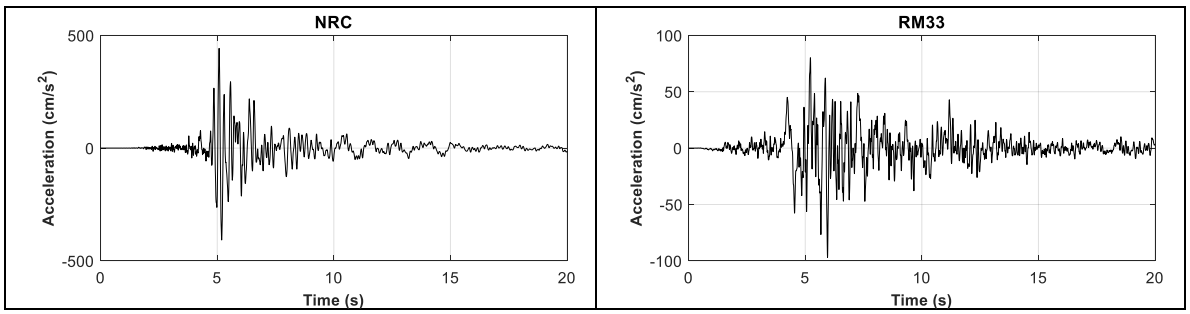

Figure 3. Fault Normal components of the acceleration time series of the selected near-fault ground motion records.

Figure 4 reports the velocity time series (black plots) of the FN components of the 6 seismic stations selected among those which recorded the strong ground motion on August 24, 2016. For each time series, the pulses (red plots) were extracted using the procedure provided by Baker [26]. This method allows to also evaluate the period T_P of the pulse. In addition, the Peak-to-Peak Velocity, given by the difference between the two peaks in one cycle of motion, was evaluated and reported for each record. This parameter can be more useful than PGV, because generally the pulses generated during near-fault strong motion are double-sided [27].

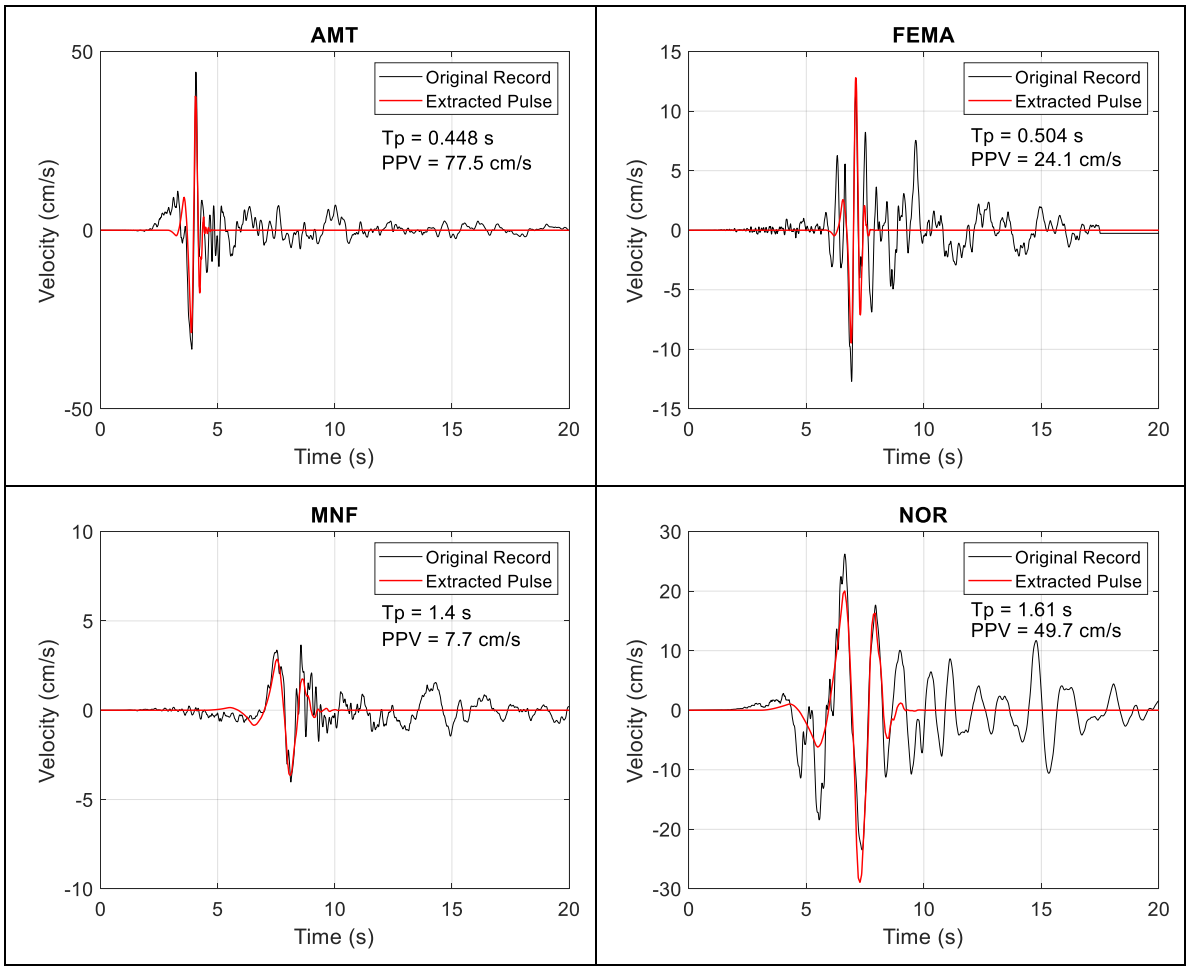

Preprints (www.preprints.org) | NOT PEER-REVIEWED | Posted: 2 September 2020 doi:10.20944/preprints202009.0023.v1

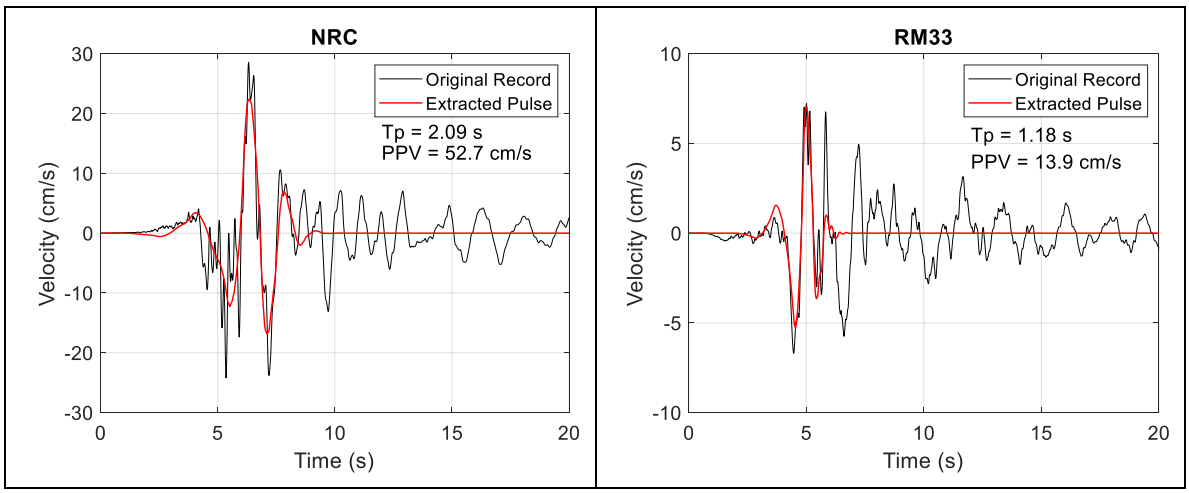

Figure 4. Velocity time series (black plots) and extracted pulses (red plots) of the FN components of the 6 seismic stations selected among those which recorded the strong ground motion on August 24, 2016

3.3. Modeling

The bridge was modelled using the finite element (FE) software SAP2000 NL, v. 21 [28] according to the structural scheme already used in previous studies [29].

The model, displayed in **Figure 5**, ideally represents the mass distribution, strength, stiffness and deformability of the real bridge; piers and girders supporting the deck were modelled by frame elements with cross section modelled according to the real geometry. The connection between the superstructure and the abutment was modeled as a rigid connection in the transversal direction. All the pier elements were modelled with nonlinear properties at the possible yield locations, i.e. plastic regions according to Eurocode 8. The plastic hinges were modelled with the fiber (P-M2-M3) hinges available in SAP2000 as suggested in [30].

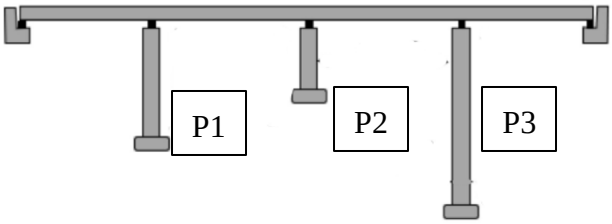

Figure 5. Bridge structural model

Unconfined and confined concrete were assigned for the concrete cover and confined for the rest of the section; the Mander's [31] concrete model was used to model confined and unconfined concrete stress-strain relationships whereas the constitutive model of the reinforcing steel was intended consistently with the design parameters of the B450C (Fy=450 Mpa, Es=210000 Mpa, Fu=540 Mpa). The fiber hinges were defined by moment-rotation curves calculated using a fiber-based model of the cross-section according to the reinforcement details at the hinge locations.

3.4 Modal properties

Modal properties of the bridge model were obtained from the linear dynamic modal analysis. **Table 3** reports the parameters of the relevant modes in transverse direction. **Figure 6** shows the bridge modal shapes in the same direction. In this work, according to what discussed in [32] only modes with a mass ratio ≥3% are considered, the others can be neglected. The participating mass ratio

Preprints (www.preprints.org) | NOT PEER-REVIEWED | Posted: 2 September 2020 doi:10.20944/preprints202009.0023.v1

of the first three relevant modes were respectively 16.9%, 71.3% and 4.5% (mode 4 was therefore almost insignificant in the elastic phase but this condition, as discussed later, changed in the nonlinear phase); the cumulative mass participating ratio for the first three modes was 92.7% (the participating mass ratio of the other modes was less than 1%). The first three mode shapes in the transverse direction have been adopted performing the MPA and mode 3 (T3=0.53s) is the dominant one.

Table 3: Bridge modal properties.

Mode	Period	Participating Mass
N°	Sec	%
1	0,65	16,9
3	0,53	71,3
4	0,13	4,5

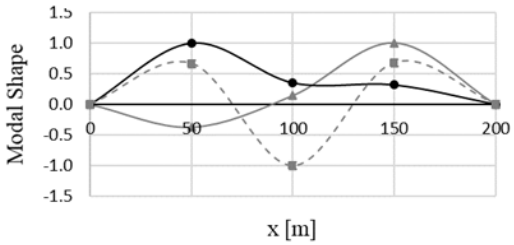

Figure 6: Bridge modal shapes (transverse direction).

4. Non-linear analyses

The bridge was analyzed at several seismic intensity levels: considering a scale factor from 0.5 to 2.0 being the average PGA of the GM selected 0.32g and being PGA=0.35g the design value of the bridge analyzed.

The dynamic analysis was performed in two steps. In the first step, a nonlinear static analysis was carried out by applying the gravity loads. The second step consisted in performing a nonlinear Response-History Analysis (NRHA) of the bridge (using time increments of 0.1 s) when subjected to all scaled ground motion records applied considering both the vertical and the transverse component of the ground motion (applied transversal to the bridge direction). All relevant modes (mode 1, 3 and 4) were taken into account [33] performing the proposed procedure. In the nonlinear direct-integration time history analysis, both material and geometric (large displacement effects) nonlinearities were considered. Among the common methods provided by SAP2000 software for conducting direct-integration time history analysis, the Hibler-Hughes-Tylor alpha (HHT) technique [34] was used in this study.

In order to enhance the accuracy, the smallest possible time-steps and alpha values close to zero were applied along with Rayleigh damping, a function of the mass and stiffness of the structure. From **Figures 7-9** the structural response to each GM is plotted in terms of deck displacement (transversal displacement of the deck at Pier 1, Pier 2 and Pier 3) and the variation of the axial load on each pier. The axial load variation is useful to evaluate the relevance of the vertical component of the GM in terms of axial load-bending moment interaction (the hinge of the piers are PM being P=axial load and M=bending moment) and therefore for the structural response; in a pushover analysis this loading variation cannot be considered adopting procedures such as SPA, UPA or MPA; all the cited pushover methods the analysis is performed starting from a preliminary non-linear step in which the vertical static loads are imposed. As already discussed in the introduction, in a preliminary phase of this work the use of EMPA (a modal pushover that includes also the vertical component of the seismic action) as an alternative to MPA was evaluated. This modification of the IMPAb was discarded because the results, using MPA or EMPA were very similar as discussed below.

Preprints (www.preprints.org) | NOT PEER-REVIEWED | Posted: 2 September 2020 doi:10.20944/preprints202009.0023.v1

As one can observe from **Figures 7-9** (only the scale factor SF=1.0 is plotted for the sake of brevity), the response to AMT record is characterized by the highest variation of the piers axial load (about ±40% of variation from the static load determined in seismic condition and used for the pushover analyses). This condition may suggest that the vertical action is relevant and therefore it can compromise results in a static pushover analysis. However this remark, that is true only for some typologies of structures and in particular only for some specific typologies of bridges (e.g. cable-stayed bridges [19]), cannot be applied to bridges, like the case study of this work, since the gravity loads influenced the design of the deck but not the pile one. In fact, the piers are usually designed with the bending action and ductility requirements (Eurocode 8 in this case [35]). Moreover, the axial load capacity is determined considering loading conditions (e.g. traffic load) that are strongly higher than the seismic vertical action. The case study analyzed is an example of this condition; **Figure 10** demonstrate that even a variation of axial load of about ±40% (that is the highest of the set of time histories selected) doesn't influence the cross section plastic behavior and therefore the capacity of the piers. This condition encourages the development and testing of pushover-based procedures also for bridges under near-fault seismic events and it justifies the good performance of IMPAb described in (§5).

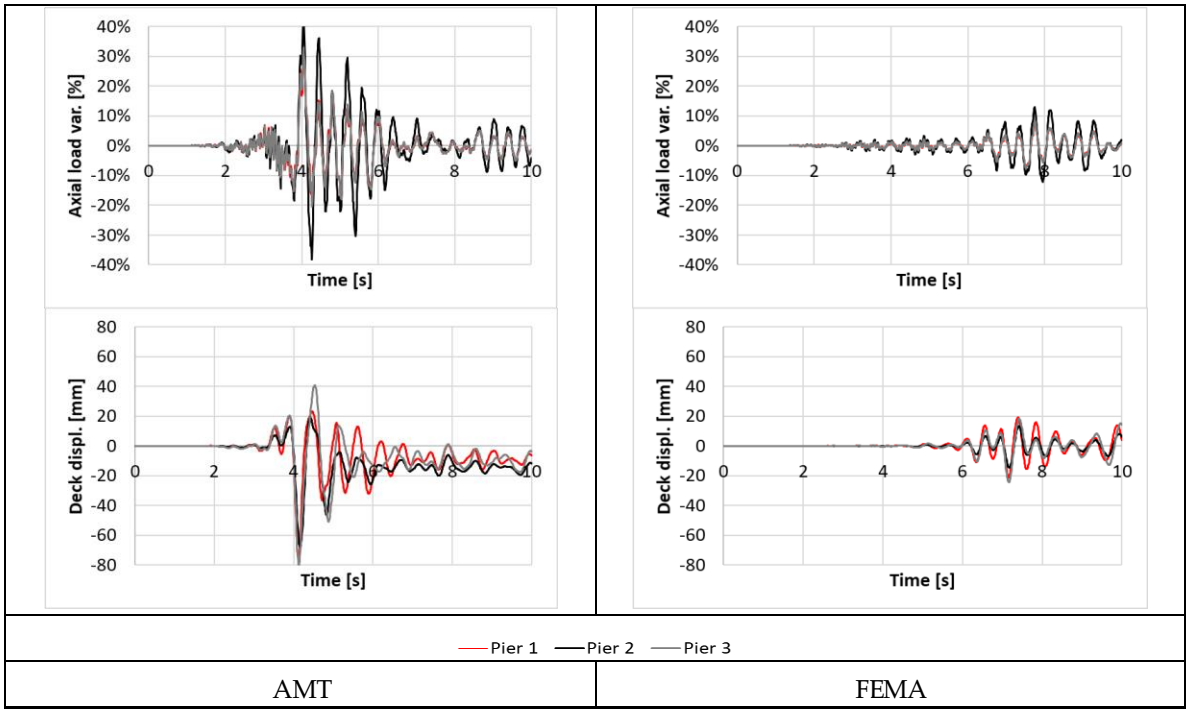

Figure 7: NRHA with scale factor 1.0 (considering both vertical and transversal components): top) Variation of the axial load (from the static load) on piers during the seismic event; bottom) Deck displacements

Preprints (www.preprints.org) | NOT PEER-REVIEWED | Posted: 2 September 2020 doi:10.20944/preprints202009.0023.v1

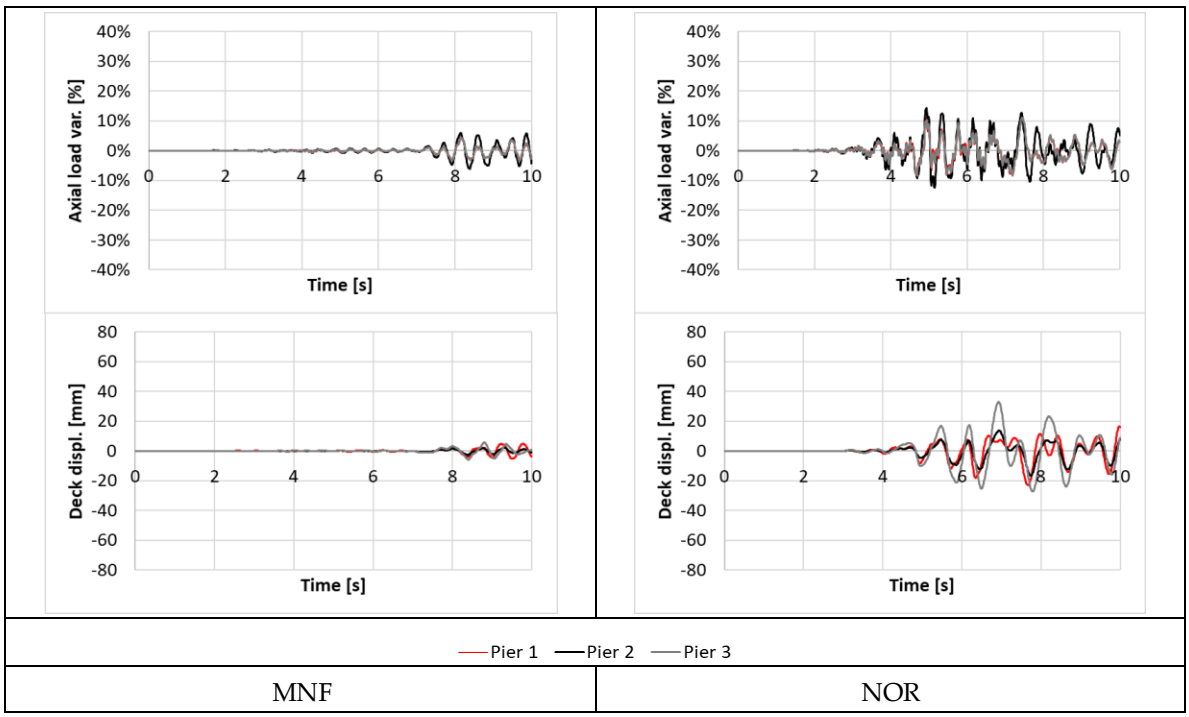

Figure 8: NRHA with scale factor 1.0 (considering both vertical and transversal components): top) Variation of the axial load (from the static load) on piers during the seismic event; bottom) Deck displacements

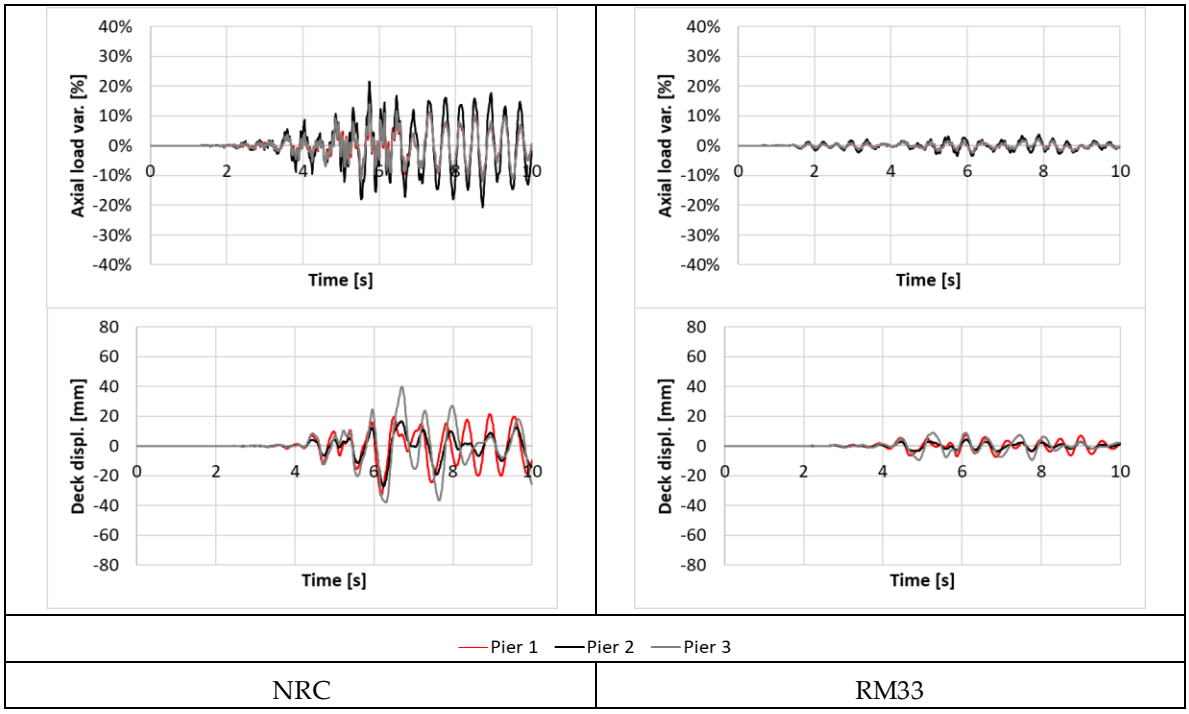

Figure 9: NRHA with scale factor 1.0 (considering both vertical and transversal components): top) Variation of the axial load (from the static load) on piers during the seismic event; bottom) Deck displacements

Preprints (www.preprints.org) | NOT PEER-REVIEWED | Posted: 2 September 2020 doi:10.20944/preprints202009.0023.v1

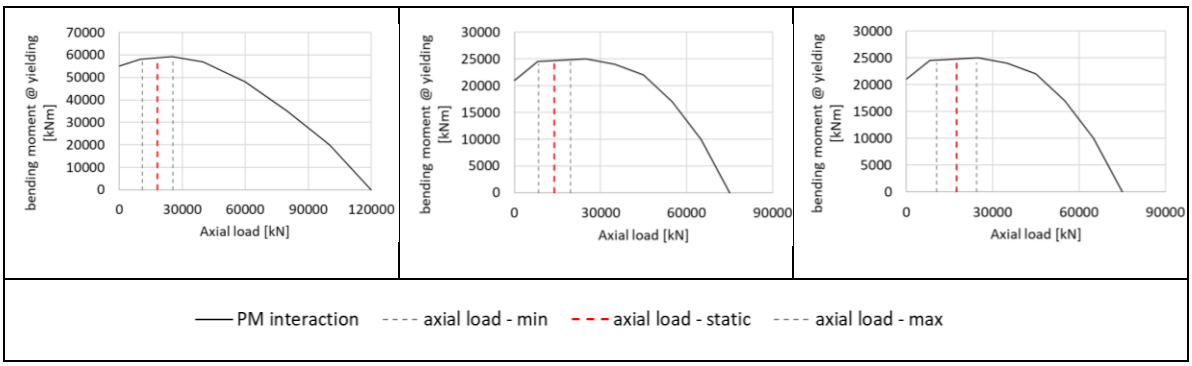

Figure 10: Axial load – bending moment @ yielding compared with a variation of axial load of ±40%. From the top: Pier 1, Pier 2 and Pier 3

In Figure 11-13 are displayed the deformed shapes of the deck when the maximum displacement of the monitoring point (P1) has been recorded. From the analysis conducted emerged that, differently to what usually happen performing NRHA with FF ground motions, with the NF events considered the structural response was characterized by a contemporary achievement of the maximum displacement of the monitoring point and the maximum global base shear. Comparing Figures 11-13 and observing Figure 14 is clear how the inelastic response, for scale factors greater than 1.0, modifies the response and the deformed shape changes becoming more uniform and less similar to a modal shape.

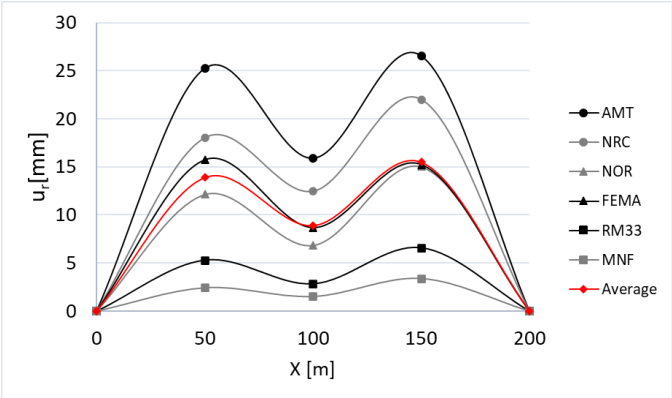

Figure 11: NRHA with scale factor 0.5 - Deck displacements

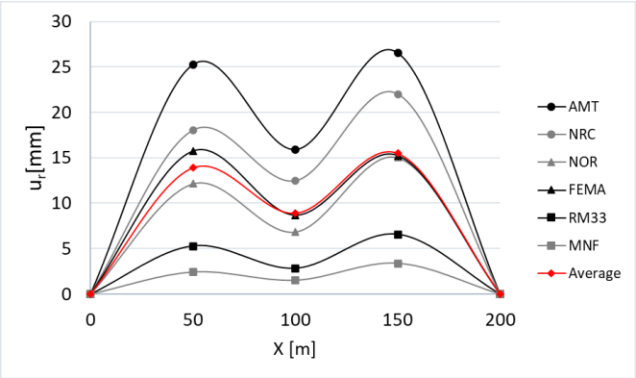

Figure 12: NRHA with scale factor 1.0 - Deck displacements

Preprints (www.preprints.org) | NOT PEER-REVIEWED | Posted: 2 September 2020 doi:10.20944/preprints202009.0023.v1

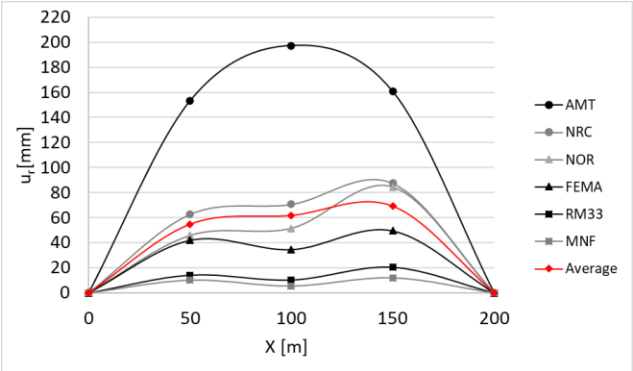

Figure 13: NRHA with scale factor 2.0 - Deck displacements

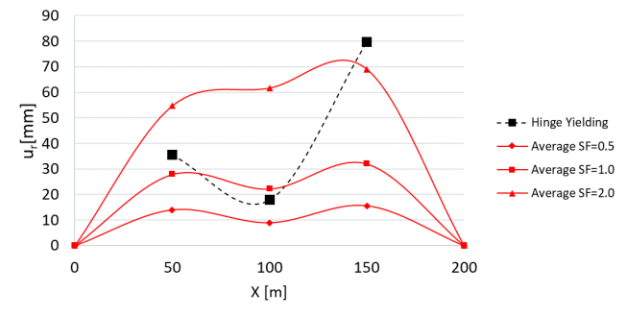

Figure 14: NRHA average response compared with displacements corresponding to plastic hinges yielding

From Figure 15 it can be observed that the results of the "standard" pushover methods (SPA and UPA) differ, even qualitatively for high intensities (SF=2.0), from the results of the NRHA and the envelope of MPA and UPA emerge as the best approach that, for an intensity level corresponding to a scale factor 1.0 and therefore to a PGA=0.32g that is very close to the bridge design intensity (PGA=0.35g), giving results similar to NRHA. In general, every pushover procedure considered underestimates the response at the center (Pier 2) and at the flexible side (Pier 3). This result is consistent to what was obtained in [17], applying IMPAb to the same case study for far field events (FF).

According to the results presented in other works considering FF events (Kappos et al. [36-37]), the application with NF events confirmed that for bridges with asymmetric modes (Mode 1 and 4) and other relevant translational modes (mode 3, the most relevant one) it is crucial the occurrence of the first plastic hinges shown in Figure 16. When the first hinge occurred in the central column the mode shape drastically changed and it should be recognized that even the multimodal method cannot reflect these sudden and substantial changes in the dynamic properties of the structure. The MPA worked relatively well also in the case of the design earthquake, when the hinge in the central column occurs. This, however, was not surprising, since the response was predominantly influenced by one mode dictated by the superstructure. All relevant modes (mode 1, 3 and 4) were taken into account performing each MPA. As it can be observed in Figure 17 (for each intensity step, the curves MPA-UPAenv are compared with the NRHA results), MPA coincided quite well with the results of NRHA up to the real average event intensity (from PGA 0.16g to PGA 0.32g) but the envelope of MPA and UPA should be considered (MPA_UPAenv) to achieve a better estimation.

For higher intensities (scale factor 2.0: PGA=0.64g) a good estimation of displacement was only observed at Pier 1, according to the experience from FF events; Figure 14 and 16 illustrates that the

Preprints (www.preprints.org) | NOT PEER-REVIEWED | Posted: 2 September 2020 doi:10.20944/preprints202009.0023.v1

first plastic hinges were in Pier 2, first, and Pier 1 after (at about PGA = 0.3g, lower than the design intensity), whereas in Pier 3 the first hinge emerged only at a very high intensity level (greater than PGA 0.64g). It was observed that a limit state (ultimate limit state at the base of Pier 2) was reached for an intensity level close to PGA 0.5g at Pier 2 and therefore, for the scope of the procedure, the investigation of higher intensities was useless.

The capacity curves of the bridge (Figure 17 and 18) were determined performing all the incremental pushover analysis tested (IMPA, ISPA, IUPA and IMPAb) and the incremental dynamic analysis IDA. The comparison confirmed a very good accuracy for IMPAb also for NF events; the response obtained with IDA was, similarly to what was observed with FF, included between IMPA and the incremental UPA (IUPA); therefore the IMPAb (envelope of IMPA and IUPA) is. Limited tro the analyzed cases, the better performing approach (the capacity curve fits the IDA' curve or, for high intensities, results are conservative).

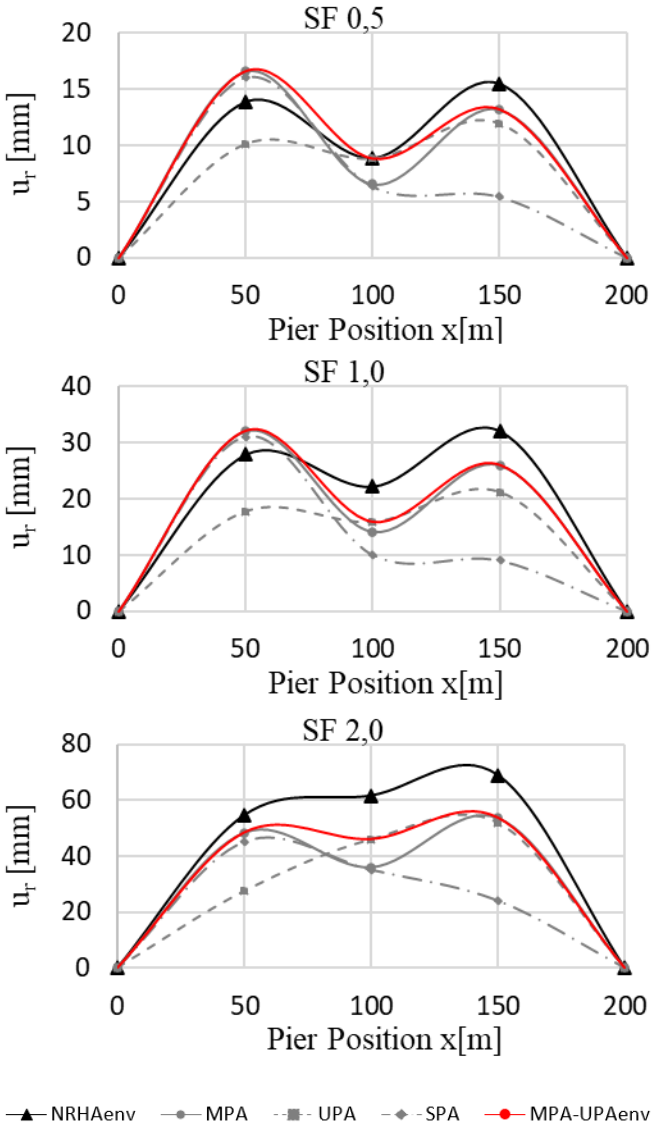

Figure 15: Fault normal: Deck displacements derived performing non-linear dynamic analysis and pushover analysis according to the approaches considered (scale factor from 0.5g to 2.0g).

Preprints (www.preprints.org) | NOT PEER-REVIEWED | Posted: 2 September 2020 doi:10.20944/preprints202009.0023.v1

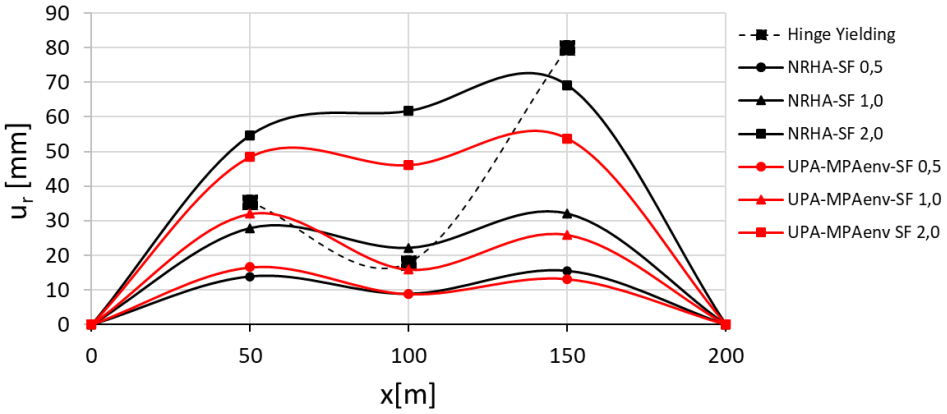

Figure 16: Fault normal: Deck displacements derived performing non-linear dynamic analysis and pushover analysis according to the approaches considered (scale factor from 0.5g to 2.0g).

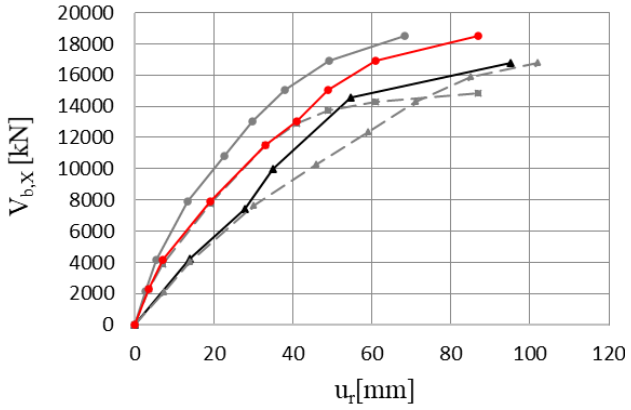

Figure 17: Case study – incremental curve and capacity curves derived with IDA or IMPAβ (the design PGA was 0.35g corresponding to a transversal base shear of Vb,x ~ 13000 kN): maximum values of u_r and Vb,x.

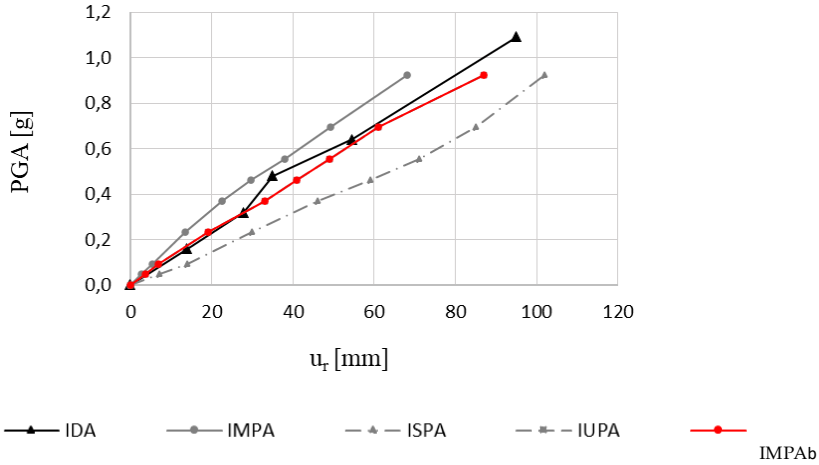

Figure 18: Case study – incremental curve and capacity curves derived with IDA or IMPAβ (the design PGA was 0.35g corresponding to a transversal base shear of Vb,x ~ 13000 kN): monitoring point displacement (Pier 1) Vs seismic intensity.

Preprints (www.preprints.org) | NOT PEER-REVIEWED | Posted: 2 September 2020 doi:10.20944/preprints202009.0023.v1

5. Conclusions

The primary objective of this paper was to verify the validity of results of an incremental (with seismic intensity) procedure performed with non-linear static analysis to estimate the seismic demands for bridge structures subjected to near-fault ground motions. The procedure IMPAb, recently developed specifically for bridges and tested with far-field events, was proved to be effective for near field too, for the irregular bridge considered.

The influence of different load patterns, including the solution proposed in IMPAb (Figure 19), on different seismic demands (deck displacement, capacity curve) were investigated in this paper. The following conclusions can be drawn from this study that is limited to a single case study and, therefore, will be followed by a more extended validation.

The application presented shows that in case of pulse-like near fault seismic events the use of MPA is equivalent to the use of EMPA (that is a modal pushover performed including the vertical seismic action). According to what was already observed also for far field events, the response evaluated with MPA, UPA (or even SPA) presents some differences. In particular, considering NF events and comparing pushover and NRHA the following considerations emerges:

- MPA overestimates the response at P1 and underestimate the response at P2 and P3.
- UPA, underestimates the response at P1 and, at P2 and P3, gives results very similar to NRHA.
- Performing IMPAb, according to the procedure originally defined (enveloping UPA and MPA) the response obtained, according to what was already observed considering FF events, is very similar to IDA, (i.e at the various intensities pushover with envelope Vs NRHA give very similar results).

Therefore, this new application of the procedure IMPAb shows a satisfactory estimation of the structural response of a bridge under near field events in terms of deck displacement for intensities up to the achievement of the first collapse (ultimate curvature achieved in a pier plastic hinge). Good results were obtained in terms of definition of the capacity curve both considering the maximum values of the displacement Vs base shear or the monitoring point displacement Vs seismic intensity.

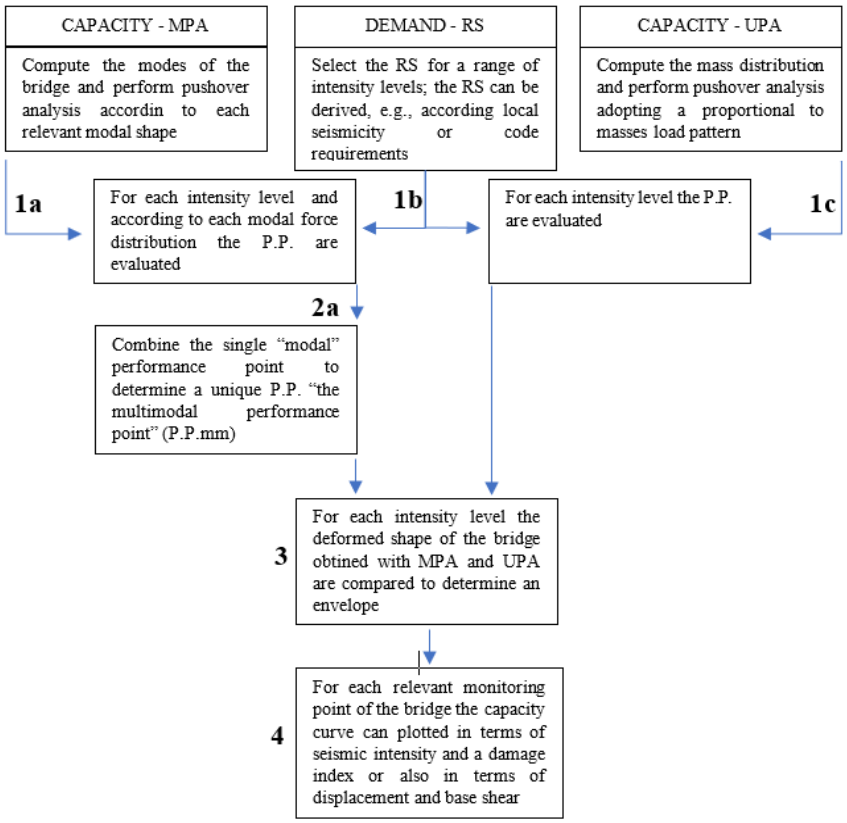

Figure 19. Flowchart of IMPAb procedure for non-linear static analysis of bridges

Author Contributions: Conceptualization, A.V.B.; methodology, A.V.B., C.N., G.F.; Resources, A.V.B, C.N., G.F. and B.B., software-analysis, A.V.B.; writing—original draft preparation, A.V.B., G.F.; writing—review and editing, A.V.B., G.F., , D.L., C.N. and B.B. All authors have contributed substantially to the work reported. All authors have read and agreed to the published version of the manuscript.

Funding: The authors gratefully acknowledge the funding received by The Laboratories University Network of Seismic Engineering (ReLUIS): research project ReLUIS/DPC 2019-2021 Reinforced Concrete Existing Structures and the National Natural Science Foundation of China [grant No. 51778148].

Conflicts of Interest: The authors declare no conflict of interest.

References

1. Papazoglou, A. J., Elnashai, A. S. (1996). Analytical and field evidence of the damaging effect of vertical earthquake ground motion. Earthquake Engineering & Structural Dynamics, 25(10), 1109-1137.
2. Bolt B, Abrahamson N. Estimation of strong seismic ground motion. In: International handbook of earthquake and engineering seismology, Vol.81B. Academic Press;2003. pp.983–1001.ATC, Applied Technology Council. Seismic Evaluation and Retrofit of Concrete Buildings; ATC 40 Report; ATC: Redwood City, CA, USA, 1996.
3. Somerville, P. G. (2002). Characterizing near fault ground motion for the design and evaluation of bridges. In Proceedings of the 3rd National Seismic Conference and Workshop on Bridges and Highways (Vol. 28, pp. 137-148).
4. Rodriguez-Marek, A., & Cofer, W. F. (2007). *Dynamic response of bridges to near-fault, forward directivity ground motions* (No. WA-RD 689.1). United States. Federal Highway Administration.
5. Somerville, P. G., Smith, N. F., Graves, R. W., & Abrahamson, N. A. (1997). Modification of empirical strong ground motion attenuation relations to include the amplitude and duration effects of rupture directivity. Seismological research letters, 68(1), 199-222.
6. Burks, L. S., & Baker, J. W. (2016). A predictive model for fling-step in near-fault ground motions based on recordings and simulations. Soil Dynamics and Earthquake Engineering, 80, 119-126.
7. Lavorato D., Vanzi I., Nuti C., Monti G. (2017) Generation of Non-synchronous Earthquake Signals. In: Gardoni P. (eds) Risk and Reliability Analysis: Theory and Applications. Springer Series in Reliability Engineering. Springer, Cham. https://doi.org/10.1007/978-3-319-52425-2_8]
8. Billah, A. M., Alam, M. S., & Bhuiyan, M. R. (2013). Fragility analysis of retrofitted multicolumn bridge bent subjected to near-fault and far-field ground motion. Journal of Bridge Engineering, 18(10), 992-1004.
9. Dicleli, M., & Buddaram, S. (2007). Equivalent linear analysis of seismic-isolated bridges subjected to near-fault ground motions with forward rupture directivity effect. Engineering Structures, 29(1), 21-32.
10. Shen, J., Tsai, M. H., Chang, K. C., & Lee, G. C. (2004). Performance of a seismically isolated bridge under near-fault earthquake ground motions. Journal of Structural Engineering, 130(6), 861-868.
11. Liao, W. I., Loh, C. H., & Lee, B. H. (2004). Comparison of dynamic response of isolated and non-isolated continuous girder bridges subjected to near-fault ground motions. Engineering Structures, 26(14), 2173-2183.
12. Vamvatsikos, D. and Cornell, C.A., "Incremental dynamic analysis", Earthquake Engineering & Structural Dynamics, 2002; 31(3), 491-514.
13. Esfahanian, A., & Aghakouchak, A. A. (2019). A single-run dynamic-based approach for pushover analysis of structures subjected to near-fault pulse-like ground motions. Journal of Earthquake Engineering, 23(5), 725-749.
14. Kalkan, E., & Kwong, N. S. (2012). Assessment of modal-pushover-based scaling procedure for nonlinear response history analysis of ordinary standard bridges. Journal of Bridge Engineering, 17(2), 272-288.
15. Bergami A.V., Forte A., Lavorato D., Nuti C. Proposal of an Incremental Modal Pushover Analysis (IMPA). Techno Press, Earthquake & Structures, Vol. 13, No. 6 (2017) 539-549, ISSN: 2092-7614 (Print).
16. Bergami, A.V., Nuti, C., Liu, X. Proposal and application of the Incremental Modal Pushover Analysis (IMPA). IABSE Conference, Geneva 2015: Structural Engineering: Providing Solutions to Global Challenges - Report pp. 1695-1700.

17. Bergami, A.V.; Nuti, C.; Lavorato, D.; Fiorentino, G.; Briseghella, B. IMPAβ: Incremental Modal Pushover Analysis for Bridges. Appl. Sci. 2020, 10, 4287.
18. Lavorato, D., Fiorentino, G., Bergami, A. V., Briseghella, B., Nuti, C., Santini, S., & Vanzi, I. (2018). Asynchronous earthquake strong motion and RC bridges response. *Journal of Traffic and Transportation Engineering (English Edition)*, *5*(6), 454-466.
19. Camara, A., Astiz, M. A. (2012). Pushover analysis for the seismic response prediction of cable-stayed bridges under multi-directional excitation. *Engineering Structures*, *41*, 444-455.
20. Goel, R.K. and Chopra, A.K. (2004). Evaluation of modal and FEMA pushover analyses: SAC buildings. Earthquake Spectra. 20(1), 225-254.
21. Paraskeva TS, Kappos AJ, Sextos AG. Extension of modal pushover analysis to seismic assessment of bridges. Earthquake Eng Struct Dynam 2006;35(10):1269–93.
22. Fiorentino, G., Forte, A., Pagano, E. et al. Damage patterns in the town of Amatrice after August 24th 2016 Central Italy earthquakes. Bull Earthquake Eng 16, 1399–1423 (2018). https://doi.org/10.1007/s10518-017-0254-z.
23. ReLUIS-INGV Workgroup (2016), Preliminary study on strong motion data of the 2016 central Italy seismic sequence V6, available at http://www.reluis.it.
24. Luzi L, Puglia R, Russo E & ORFEUS WG5 (2016). Engineering Strong Motion Database, version 1.0. Istituto Nazionale di Geofisica e Vulcanologia, Observatories & Research Facilities for European Seismology. doi: 10.13127/ESM.
25. Luzi, L., Pacor, F., Puglia, R., Lanzano, G., Felicetta, C., D'Amico, M., ... & Baltzopoulos, G. (2017). The central Italy seismic sequence between August and December 2016: Analysis of strong-motion observations. Seismological Research Letters, 88(5), 1219-1231.
26. Baker, J. W. (2007). Quantitative classification of near-fault ground motions using wavelet analysis. Bulletin of the Seismological Society of America, 97(5), 1486-1501.
27. Hayden, C. P., Bray, J. D., & Abrahamson, N. A. (2014). Selection of near-fault pulse motions. Journal of Geotechnical and Geoenvironmental Engineering, 140(7), 04014030.
28. Lavorato D, Fiorentino G, Pelle A, et al. A corrosion model for the interpretation of cyclic behavior of reinforced concrete sections. Structural Concrete. 2019;1–15. https://doi.org/10.1002/suco.201900232
29. Liu, T., Zordan, T., Zhang, Q., & Briseghella, B. (2015). Equivalent viscous damping of bilinear hysteretic oscillators. Journal of Structural Engineering, 141(11), 06015002.
30. Lavorato, D., Fiorentino, G., Bergami, A.V., Ma, H.-B., Nuti, C., Briseghella, B., Vanzi, I., Zhou, W. Surface generation of asynchronous seismic signals for the seismic response analysis of bridges. 6th International Conference on Computational Methods in Structural Dynamics and Earthquake Engineering. Rhodes Island; Greece; June 2017, Volume 1, 2203-2213.
31. Mander, J. B., Priestley, M. J. N., and Park, R. (1988). "Theoretical stress–strain model for confined concrete." J. Struct. Eng., 114(8), 1804–1826.
32. Paraskeva TS, Kappos AJ. Seismic assessment of complex bridges using an improved modal pushover analysis procedure. Fifth European Workshop on the Seismic Behaviour of Irregular and Complex Structures, Catania, 16–17 September 2008; 335–348.
33. American Association of State Highway and Transportation Officials (AASHTO). Guide Specifications for LRFD Seismic Bridge Design, 2nd ed.; AASHTO: Washington, DC, USA, 2011.
34. California Department of Transportation. Caltrans Seismic Design Criteria (SDC), V1.7; California Department of Transportation: Sacramento, CA, USA, 2016.
35. European Committee for Standardization. *Eurocode 8—Design of Structures for Earthquake Resistance—Part 2: Bridges*; European Committee for Standardization: Brussels, Belgium, 2005.
36. Kappos A. J., Goutzika E. D., Stefanidou S. P., Sextos A. G.. Problems in Pushover Analysis of Bridges Sensitive to Torsion. Computational Methods in Applied Sciences 21, 2010. DOI 10.1007/978-94-007-0053-6_5,
37. Kappos AJ, Paraskeva TS. Nonlinear static analysis of bridges accounting for higher mode effects. Workshop on Nonlinear Static Methods for Design/Assessment of 3D Structures, Lisbon, Portugal, 2008.